Comparative studies of silicon photomultipliers and traditional vacuum photomultiplier tubes*

SHI Feng(石峰)[1,2;1)] LÜ Jun-Guang(吕军光)[1] LU Hong(卢红)[1] WANG Huan-Yu(王焕玉)[1]
MA Yu-Qian(马宇蒨)[1] HU Tao(胡涛)[1] ZHOU Li(周莉)[1] CAI Xiao(蔡啸)[1] SUN Li-Jun(孙丽君)[1]
YU Bo-Xiang(俞伯祥)[1] FANG Jian(方建)[1] XIE Yu-Guang(谢宇广)[1] AN Zheng-Hua(安正华)[1]
WANG Zhi-Gang(王志刚)[1] GAO Min(高旻)[1] LI Xin-Qiao(李新乔)[1] XU Yan-Bing(徐岩冰)[1]
WANG Ping(王平)[1] SUN Xi-Lei(孙希磊)[1,2] ZHANG Ai-Wu(章爱武)[1,2] XUE Zhen(薛镇)[1,3]
LIU Hong-Bang(刘宏邦)[2] WANG Xiao-Dong(王晓东)[1,4] ZHAO Xiao-Yun(赵小芸)[1,2]
ZHENG Yang-Heng(郑阳恒)[2] MENG Xiang-Cheng(孟祥承)[1] WANG Hui(王辉)[1]

[1] Institute of High Energy Physics, CAS, Beijing 100049, China
[2] Graduate University of Chinese Academy of Sciences, Beijing 100049, China
[3] University of Science and Technology of China, Hefei 230026, China
[4] Shanxi University, Taiyuan 030006, China

Abstract: Silicon photomultipliers (SiPMs) are a new generation of semiconductor-based photon counting devices with the merits of low weight, low power consumption and low voltage operation, promising to meet the needs of space particle physics experiments. In this paper, comparative studies of SiPMs and traditional vacuum photomultiplier tubes (PMTs) have been performed regarding the basic properties of dark currents, dark counts and excess noise factors. The intrinsic optical crosstalk effect of SiPMs was evaluated.

Key words: silicon photomultiplier, SiPM, PMT, dark current, dark counts, excess noise factor

PACS: 29.40.-n, 29.40.Wk, 85.60.-q **DOI:** 10.1088/1674-1137/35/1/011

1 Introduction

The development of photodetectors sensitive to low-intensity photon flux is one of the critical issues for particle and nuclear physics experiments. It became possible almost 80 years ago when the first photomultiplier tube (PMT) was invented at RCA laboratories and it became a commercial product in 1936 [1]. However, as standard photodetectors, PMTs have two main obstacles: they are very sensitive to magnetic fields and their prices are high due to their complicated production process. The search for an alternative to PMT started a long time ago. One of the most promising candidates was the multipixel Geiger-mode Avalanche Photodiode (G-APD), which is capable of detecting single photons like a PMT and was thereby called a silicon photomultiplier (SiPM) [2]. The first G-APDs were studied for photon detection in the early 1960s [3–5]. Around the beginning of this millennium, significant progress was made by Russian groups in the development of SiPMs. They have the advantages of high gain (10^5–10^6) and photon detection efficiency, excellent photon-counting capability and single photon timing resolution, room temperature and low bias operation, insensitivity to magnetic fields, compactness, robustness and anticipated low cost for mass production. These characteristics are very attractive for possible domestic projects of spaceborne instrument developments, where the weight, volume and power consumption are critically restricted. To understand these novel devices, which may be used as substitutes for traditional PMTs in particle detectors, a series of laboratory tests have been performed. In this paper, we focus on the basic properties of dark currents, dark counts and excess noise factors of the SiPMs at room

Received 18 March 2010, Revised 9 April 2010
* Supported by National High Technology Research and Development Program of China (2007AA12Z133)
1) E-mail: shif@ihep.ac.cn

temperature since these are crucial considerations for space applications. The corresponding performance of a traditional vacuum PMT was tested for comparison.

2 Operation principle

The SiPM is a combination of a large number of identical silicon APD microcells (pixels) on a common substrate, electrically connected in parallel and operated in limited Geiger mode with an integrated quenching mechanism [6–8]. Typical pixel densities are 100–1600 pixels per mm^2 with pixel dimensions from 25 μm×25 μm to 100 μm×100 μm. The spectral response range for incident photons extends from 270 nm to 900 nm with the peak photon detection efficiency (PDE) of about 40% (typical). The typical structure of a G-APD microcell is of the well-known "reach through avalanche structure", with layers of n^+-p-π-p^+ fabricated on a p-type epitaxial contact[1)] [9]. Incident photons are absorbed and converted to photo-stimulated electron-hole pairs mainly in the lightly p-type doped π-layer. An avalanche of ionization process can be induced by the primary carriers of drift electrons with certain probabilities in the "needle" n^+-p junction [10]. Since the reverse bias is above the breakdown voltage for 10%–20% higher, the gain of the Geiger mode charge multiplication amounts to 10^6. Therefore each G-APD microcell acts as a binary device with a single photon counting capability. Moreover, the output signal is the sum of the signals from all of the microcells firing at the same time, the SiPM becomes globally an analog device like a PMT. A problem of the SiPMs is the optical crosstalk between the neighboring G-APD microcells, which prevents the microcells from independent photon counters. This originates from photons created in the Geiger discharge with a rate of about 3×10^{-5} photons per avalanche electron [11]. These photons may propagate to another not primarily fired pixel and initiate an additional discharge there.

3 Study of the performance and properties

Two independent sets of SiPM samples were tested. They were the multi-pixel photon counters (MPPCs) manufactured by Hamamatsu Photonics, Japan and the solid-state photomultipliers (SSPMs) from Photonique SA, Switzerland. The MPPC devices have 1 mm×1 mm and 3 mm×3 mm active areas with different numbers of pixels. They are of 3 mm×3 mm and 900 pixels (S10362-33-100C), 1 mm×1 mm and 400 pixels (S10362-11-50C), and 1 mm×1 mm and 100 pixels (S10362-11-100C) while the suggested PDEs are about 65%, 50% and 65%, respectively, at the peak sensitivity wavelength of 400 nm. The SSPM (0701BG) devices have an octagonal active area of 1.0 mm^2, with a pixel number of 556. The peak PDE is about 40% at 560 nm. Since one pixel signal on a 50 Ω load corresponds to a pulse amplitude of ∼1 mV (for a typical 10–20 ns pulse), a commercial available preamplifier (Photonique AMP_0604) with a gain of about 20 was used for the appropriate level of SiPM signals. A digital phosphor oscilloscope (TEK TDS3034C) and a standard CAMAC QDC (PHILIPS 7166) with a conversion gain of 125fC/channel were used to measure the amplitude and charge integration of the signals. A traditional vacuum PMT (XP2020) with a sensitive photocathode of 44 mm in diameter from Philips Photonics was tested as a comparative photodetector.

3.1 Operating point

The SiPM gain (G) is determined by the charge (Q) that can be released from a microcell capacitance after the breakdown,

$$G=\frac{Q}{e}=\frac{\Delta V\cdot C_{\text{microcell}}}{e}, \tag{1}$$

where $C_{\text{microcell}}$ is the microcell capacitance, e is the electron charge and ΔV is the overvoltage above the breakdown voltage ($V_{\text{breakdown}}$), which is often referred to as the operation point of an individual SiPM,

$$\Delta V=V_{\text{bias}}-V_{\text{breakdown}}. \tag{2}$$

From Eq. (1), one can easily deduce that the gain increases linearly with the overvoltage, while a larger bias voltage (V_{bias}) also increases the photon detection efficiency as well as the dark count rates and intrinsic optical crosstalk (see Section 3.4). As a result, our determination of the optimized operation point comes from the trade-off between the gain, the photon detection efficiency, the dark rate and the optical crosstalk rate. They are ΔV=0.9–1.7 V for the MPPCs and ΔV=2.0–3.2 V for the SSPMs. Note that they are also individual sample dependent.

3.2 Dark current

Since the operation voltages for the SiPMs are no more than 100 V, the power consumption of the de-

[1)] UV/blue light enhanced G-APD microcells are based on p^+-p-n^+ (n-type) structure.

vice is limited by the dark current. A picoammeter (KEITHLEY 6485) connected in series in the power supply loop was used for the static current measurement in a completely dark state. The I-V dependence of the MPPC and the SSPM samples at room temperature are shown in Fig. 1(a), (b). The measurement results are shown in Table 1. The typical dark currents are no more than 10 μA at appropriate overvoltages. As a result, the static power dissipations are less than 0.1 mW for both the MPPC and the SSPM devices. Similar measurement of the PMT is shown in Fig. 1(c), where the dark currents of 2–3 orders lower, $I_{\rm dark}$ ∼0.1–10 nA, are observed. Note that the much higher dark currents of the SiPMs mainly originate from very high rates of the intrinsic dark counts (see Section 3.4).

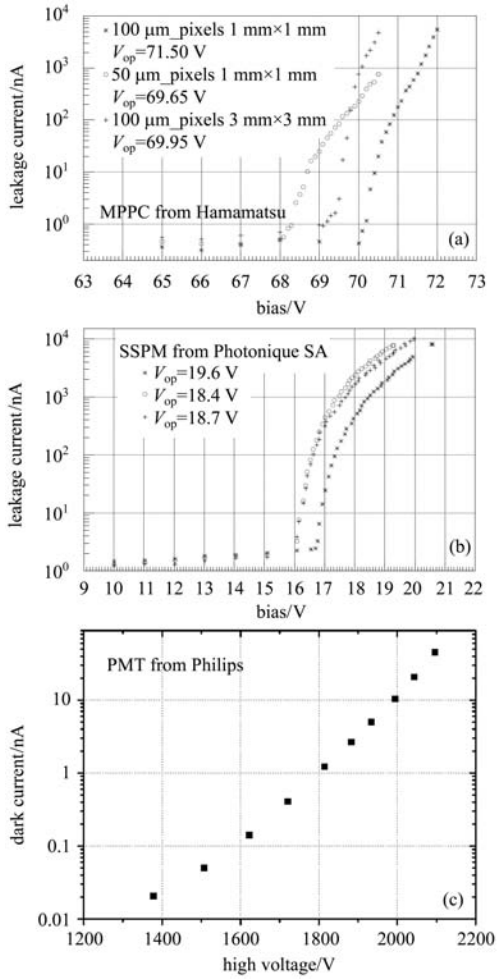

Fig. 1. Dark currents of MPPCs from Hamamatsu (a), and SSPMs from Photonique (b) in dependence on the supplied bias voltages[1)] at room temperature; (c) dark currents of a PMT (XP2020) from Philips in dependence on the supplied high voltages at room temperature.

3.3 Dark count spectrum

The electronic noise levels of the SiPMs are measured to be negligibly small, about 10% of the signals from one photoelectron (p.e.), due to the very high gain (∼10^6). Therefore, the main source of noise which determines the lower limit of light detection is the dark counts. These are composed of the primary pulses triggered by carriers thermally generated or field-assisted in the sensitive volume and the afterpulses caused by trapped carriers and their subsequent release [12].

The measurement was performed by the SSPM samples in a completely dark state, and the signal amplitudes were recorded by an oscilloscope. The dark count spectrum of a SSPM at room temperature with overvoltage ΔV=3 V is shown in Fig. 2(a). The successive peaks corresponding to 1–4 primary carriers, which can be regarded as intrinsic generated "seeds" to initiate Geiger discharge in silicon microcells without ambient photon incidence, are clearly distinguishable. This implies that a single pixel signal may cause 1–4 fired pixels with different probabilities by the effect of intrinsic optical crosstalk. But this is not always a defect. Since the thermal- or photogenerated primary carriers behave identically in the SiPMs, the unique dark count spectra can be used as a self-calibration tool in order to monitor the detector gain as environmental conditions change, which is especially important for possible space applications. The dark count spectrum of a PMT at the same condition with HV=2003 V is shown in Fig. 2(b). No successive peak is visible besides the leftmost peak due to thermionic emission of electrons from the photocathode as the majority of the constituent. It should be noted that, unlike the SiPMs, the peak position in the dark count spectrum of PMTs may differ slightly from that of single p.e. in statistics [13], thereby being inapplicable for a precise calibration of gain.

3.4 Dark rate

According to the above discussions, dark counts in the SiPMs behave mainly as pulses of single p.e. This is the main source of noise that limits the multiphoton resolution. In addition, the intrinsic optical crosstalk pulses violate the pixel independence and lead to a nonlinear response of photon-counting behavior. Therefore the dark count rates and optical crosstalk rates are crucial parameters in determining the device characteristics. It is reported that the dark

[1)] The $V_{\rm op}$ values represent factory recommended operation biases.

Table 1. Breakdown voltages, overvoltages and corresponding dark currents of the MPPC and SSPM samples at room temperature.

parameters	units	MPPC1	MPPC2	MPPC3	SSPM1	SSPM2	SSPM3
active area	mm^2	1.0	1.0	9.0	1.0	1.0	1.0
number of pixels	–	100	400	900	556	556	556
breakdown voltage	V	70.0	68.1	69.1	16.6	15.9	15.9
overvoltage	V	1.5	1.5	0.9	3.05	2.54	2.80
dark current	μA	0.78	0.12	0.76	3.69	3.76	3.48
static power dissipation	μW	56.1	8.16	53.2	72.5	69.3	65.1

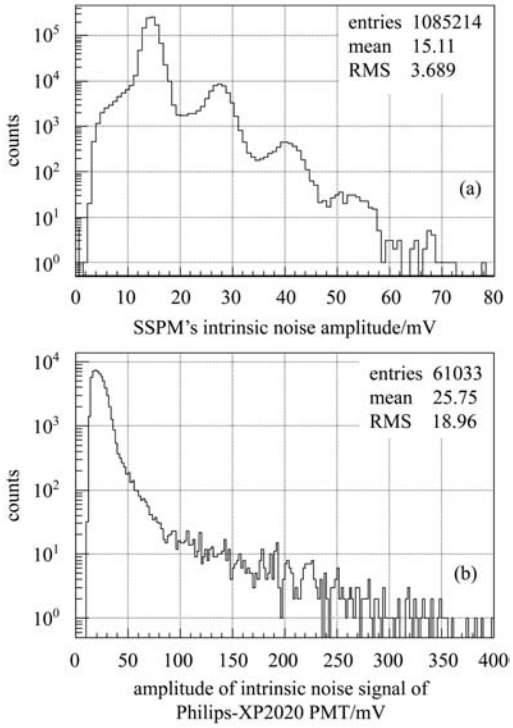

Fig. 2. (a) Dark count spectrum of a SSPM (Photonique 0701BG) operated at ΔV=3 V; (b) dark count spectrum of a PMT (Philips XP2020) operated at HV=2003 V.

rates of SiPMs amount to a few (typical 1–2) MHz/mm^2 at room temperature [14]. To verify the value, the dark rates of the MPPC and the SSPM samples in dependence on the bias voltages are measured at room temperature, as shown in Fig. 3(a), (b). Two thresholds are set to figure the dark counts as the dark rates (threshold at 0.5 p.e. equivalent) and the optical crosstalk rates (threshold at 1.5 p.e. equivalent). The optical crosstalk coefficient $K_{2/1}$, defined as the probability of a second pixel being fired by one primary carrier, was measured as a function of the overvoltage, as shown in Fig. 4(a) and (b) for the MPPC and the SSPM devices, respectively. The average dark rate and optical crosstalk rate are about 1.9 MHz/mm^2 and 0.21 MHz/mm^2, coincident with the published data [14]. The dark rate of the SSPMs is about 1.6 times higher than that of the MPPCs, but the MPPC devices have a higher rate of optical crosstalk along with a $K_{2/1}$ coefficient 3 times larger than that for the SSPMs on average. For comparison, the dark rates of a PMT as a function of supplied high voltage at room temperature are presented in Fig. 3(c). They are less than 100 Hz for a variety of voltage supplied. Note that the dark rates of the

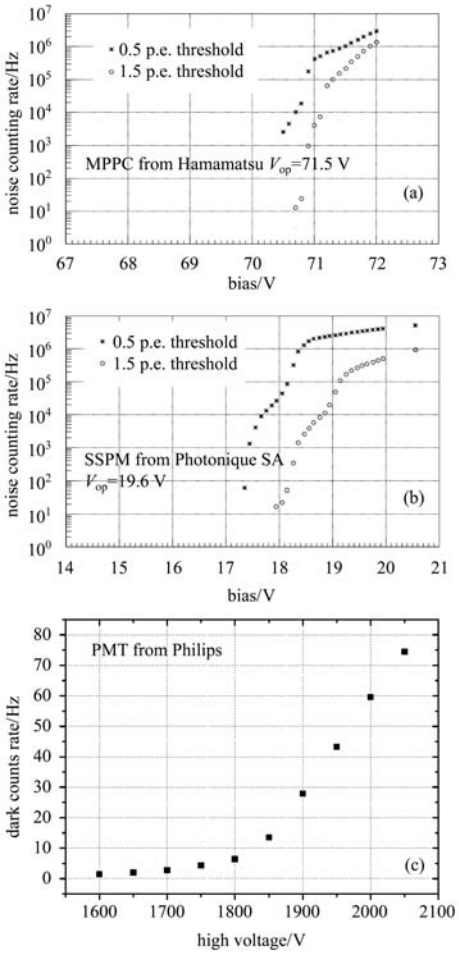

Fig. 3. Dark count rates and optical crosstalk rates of a MPPC (Hamamatsu S10362-11-100C) (a) and a SSPM (Photonique 0701BG) (b) in dependence on the supplied bias voltages at room temperature; (c) dark count rates of a PMT (Philips XP2020) in dependence on the supplied high voltages at room temperature.

SiPMs are about 4–5 orders higher than those of the PMT. We think this is one of the major problems that prevent the SiPMs from having massive applications as for the current status of the PMTs.

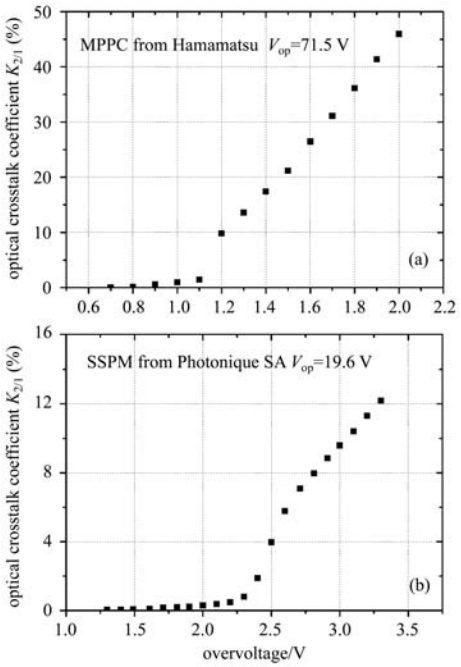

Fig. 4. Optical crosstalk coefficients ($K_{2/1}$) of a MPPC (Hamamatsu S10362-11-100C) (a) and a SSPM (Photonique 0701BG) (b) in dependence on the supplied overvoltages at room temperature.

3.5 Excess noise factor

The photon counting capability is very important for extremely low light intensity applications. It can be evaluated by the excess noise factor (ENF) parameter. The ENF describes the grade that the single photoelectron resolution is spoiled by the fluctuation in charge multiplication process in a photomultiplier (PM) and can be calculated from the width of single photoelectron spectrum as [15]

$$\mathrm{ENF} \equiv \frac{\sigma^2_{\mathrm{Output}}}{\sigma^2_{\mathrm{Input}}} = 1 + \frac{\sigma^2}{M^2}, \tag{3}$$

where M refers to the mean gain of a PM and σ^2 is the variance of the gain.

The experimental setup to measure the faint light response of the SSPM and the PMT is shown in Fig. 5(a). A light emitting diode (Nichia LED-NSPB320BS-E) was used as the light source. A light attenuator was placed between the LED and the SSPM (or the PMT) to reduce the light intensity to photon-counting level. Various LED light emissions were tuned in order to have a single photoelectron and a many photon response of the photodetectors. The LED driving pulses were adjusted to have a 1 ns rise time and 10 ns width, and the QDC gate width was set to be 50 ns so as to eliminate dark count contamination, particularly for the SSPM measurement. A typical oscilloscope waveform of the SSPM response to a few photons is presented in Fig. 5(b). The multi-photoelectron pulse charge spectra obtained by the SSPM and the PMT under illumination of extremely weak light are presented in Fig. 6(a), (b). The spectra envelopes satisfy Poisson statistics and the peaks correspond to various photoelectrons. For the SSPM, the successive 1–8 photoelectron peaks demonstrate an excellent photon-counting capability (see Fig. 6(a)), while for the PMT only 1–3 photoelectrons can be identified (see Fig.6 (b)). The ENF parameters were calculated to be 1.05 and 1.20 for the SSPM and the PMT, respectively. An invisible negative pedestal in the QDC spectrum (see Fig. 6(a)) is expected for positive drift of the signal base line. This is due to AC coupling of the output signals and high dark rates of the SSPM device.

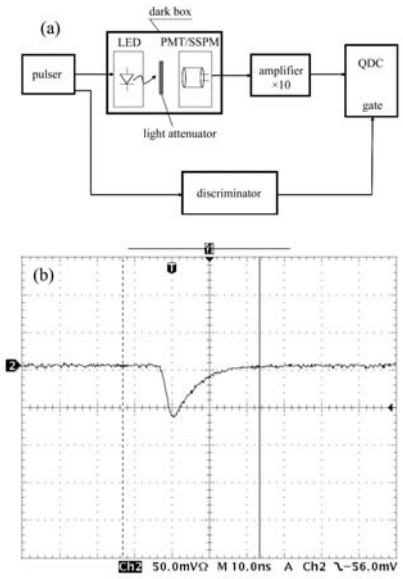

Fig. 5. (a) Schematic view of the experimental setup for LED spectra measurement; (b) typical SSPM waveform under illumination of few photons.

The great difference in the ENF values for the SiPM and PMT devices comes from the fact that different charge amplification mechanisms function. The very small ENF of the SiPM is mainly due to the Geiger mode operation of each avalanche microcell which avoids large avalanche fluctuations in proportional mode as the case in an APD. Even so, optical crosstalk acts as shower fluctuations introducing an excess noise factor and little gain variation

among pixels contributes to output charge fluctuations. These stochastic processes prevent the ENF of SiPMs from eventually being one. On the other hand, the large ENF for PMTs is mainly due to fluctuations in the charge multiplicative dynode system. Lombard and Martin [16] showed for an ideal PMT, of which all stages obey Poisson statistics and the electronics noise is negligible, that the first stage of multiplication is the most important when resolution is concerned. If the gain of the first stage is sufficiently high (>5), then the subsequent stages will have negligible effect on the dispersion of the anode signals. In this case, the ENF can be approximated to the well-known expression

$$\mathrm{ENF}=1+\frac{1}{\delta_1}+\frac{1}{\delta_1\cdot\delta_2}+\cdots+\frac{1}{\delta_1\cdot\delta_2\cdots\delta_n}\approx\frac{1+\delta_1}{\delta_1}, \quad (4)$$

where δ_1, δ_1,...,δ_n are the gains at the first, second and last stage dynodes. Therefore it is clear that the limited gain of the first dynode, no greater than 10 for ordinary, is the main cause of large ENF for the PMTs. So far, the excellent photon counting capability of the SiPMs and the poorer performance of the PMTs are quite reasonable.

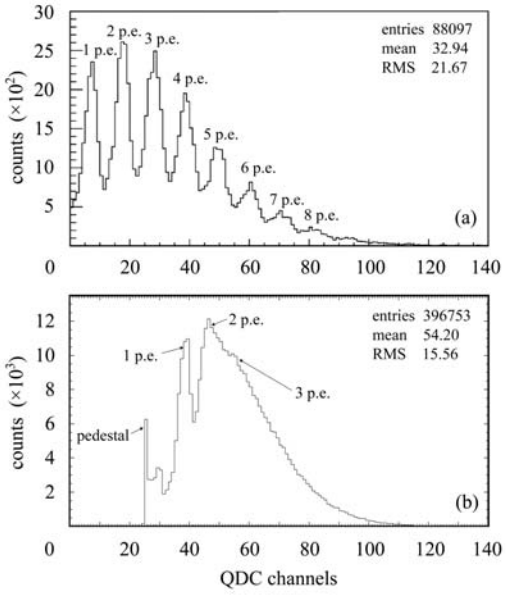

Fig. 6. Multi-photoelectron pulse charge spectra obtained by a SSPM (Photonique 0701BG) (a) and a PMT (Philips XP2020) (b).

4 Summary

SiPMs are beginning to compete with traditional vacuum PMTs. In this work, we present comparative studies to characterize the new devices of SiPMs from the different manufacturers of Hamamatsu Photonics and Photonique SA. Excellent performance of the SiPMs, such as superb single photon resolution (very small excess noise factor of about 1.05), high gain (~10^6) and low power consumption (<0.1mW) were verified. Meanwhile, the obvious drawbacks including very high dark rates (~1.9 MHz/mm^2) and intrinsic optical crosstalk rates (~0.21 MHz/mm^2) were measured at room temperature. The results are coincident with the measurement data published by international investigators. Other property comparisons between SiPMs and PMTs, such as the "sub-photoelectron" effect, transit time spread (TTS) of single photoelectron and in flight real time gain calibration methods, etc. will be reported in future work. It is believed that the development of SiPMs started some 10 years ago, but still there is plenty of room for future improvement in space applications.

The authors would like to acknowledge Dr. David McNally of Photonique SA for timely suggestions on the operation of SSPMs and Prof. Xie Yigang and Prof. Stefano Miscetti of INFN for various helpful discussions. We would like to thank the National High Technology Research and Development Program of China for its support.

References

1 Renker D. Nucl. Instrum. Methods A, 2004, **527**: 15–20
2 Ninkovic J. Nucl. Instrum. Methods A, 2007, **580**: 1020–1022
3 McIntyre R J. J. Appl. Phys., 1961, **32**(6): 983–995
4 Goetzberger A et al. J. Appl. Phys., 1963, **34**(6): 1591–1600
5 Haitz R H et al. J. Appl. Phys., 1964, **35**(5): 1370–1376
6 Dolgoshein B et al. Nucl. Instrum. Methods A, 2003, **504**: 48–52
7 Golovin V. Patent No. RU 2142175, 1998
8 Sadygov Z. Patent No. RU 2102820, 1998
9 Tsang W T (Ed.). Semiconductors and Semimetals, Volume 22, Part D: Photodetectors. New York: Academic Press, 1985
10 Saveliev V, Golovin V. Nucl. Instrum. Methods A, 2000, **442**: 223–229
11 Andreev V, Balagura V, Bobchenko B et al. Nucl. Instrum. Methods A, 2005, **540**: 368–380
12 Renker D. Nucl. Instrum. Methods A, 2006, **567**: 48–56
13 MENG Xiang-Cheng, YANG Chang-Gen et al. Nuclear Electronics & Detection Technology, 2005, **25**(6): 594–600 (in Chinese)
14 Dolgoshein B et al. Nucl. Instrum. Methods A, 2006, **563**: 368–376
15 Musienko Y. Nucl. Instrum. Methods A, 2009, **598**: 213–216
16 Lombard F J, Martin F. Rev. Sci. Instr., 1961, **32**(2): 200–201